High-T$_c$ SQUIDs Magnetocardiography Systems

Hong-Chang Yang[a], Shu-Yun Wang[a], J.C. Chen[a], M.J. Chen[a], C.S. Wu[a], H.E. Horng[b],
Shu-Hsien Liao[b] and Jen-Tzong Jeng[c]

[a] Department of Physics, National Taiwan University, Taipei, Taiwan
Fax: 886-2-23675267, e-mail: hcyang@phys.ntu.edu.tw
[b] Department of Physics, National Taiwan Normal University, Taipei, Taiwan
Fax: 886-2-88631954, e-mail: phyfv001@scc.ntnu.edu.tw
[c] Department of Mechanical Engineering, National Taipei University of Technology, Taipei, Taiwan

In general, the ambient magnetic noises are composed of many different disturbances with distinct frequency components in space in the unshielded magnetocadioography (MCG) imaging system. Besides, these electromagnetic disturbances are with different frequencies and are not homogeneous in space. Therefore, it is impossible to eliminate the noises by the simple subtraction circuit due to the attenuation factor of each frequency component of the ambient noise would be distinct. In this paper we develop a fast Fourier transform (FFT) technique to optimize the environmental noises of high-T$_c$ electronic rf SQUID magnetocardiography system. Using the FFT of three magnetometers with the Hanning window overlapped, we optimized the parameters required for the subtraction circuit in order to minimize the environmental noises in the frequency ranges of interest. Using the optimized parameters, low pass and notch filters, we reduced the environmental noise level much lower than the signal of the MCG. Hence, we can perform MCG measurements in a magnetically unshielded environment.
Key words: SQUID, MCG, magnetocardiography

1. INTRODUCTION

The magnitude of the magnetocardiography (MCG) signal, which is about 50 ~ 100 pT, is extremely weak. The ambient magnetic field noise is several orders of magnitude higher than the MCG signal. Hence, measurements of biomagnetic field are often performed inside a magnetically shielded room. Nevertheless, the magnetic shielded room is too expensive for widespread applications of the MCG. Until recently first- and second- order high-T$_c$ gradiometers, measuring the axial or the tangential fields, were demonstrated [1-2] and MCG signals were recorded in magnetically unshielded environment [3-5] or moderate shielded environments [6-8].

Usually the environmental noises can be quite complicated. The amplitude and the phase of the ambient noises are distinct at different sites and the field spectra of the magnetometers are not the same. Therefore, it is not quite easy to suppress the environmental noises. The objective of the present paper is to establish a systematic fast Fourier transform (FFT) technique to suppress the environmental noises for electronic 2nd-order gradiometer for the MCG measurements in the magnetically noisy and unshielded sites. We analyze the FFT signals of the three magnetometers, which include the information of both the amplitude and the phase. With this information, we could minimize the ambient noise in the frequency range we concerned. In other words, the more uniform the surrounding noise is, the lower the noise level of the gradiometer can be achieved. Moreover, we apply a low-pass filter and a notch filter with the frequency of the power line source in order to further reduce the environmental disturbances. Hence, the noise level of

the surrounding disturbances is much reduced so that we can perform the MCG measurement in the unshielded environment.

2. EXPERIMENTAL DETAILS

2.1 System Design

In this work, we setup a 2nd-order gradiometer, which consists of three commercially available high-temperature rf SQUID magnetometers. These three magnetometers are set up in off-axially arrangement with their sensing plane oriented along the z-axis. The vertical distance between each sensor is 6 cm, i.e. the sensing SQUID is located close to the bottom of the dewar and the other two reference SQUIDs are mounted
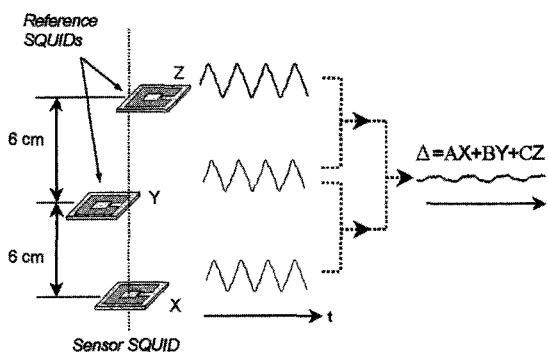

Figure 1   Configuration of the 2nd order off-axis electronic gradiometer. The vertical distance between each sensor is 6 cm. The sensing SQUID is located close to the bottom of the dewar while the other two reference SQUIDs are mounted at 6 cm and 12 cm above the sensing SQUID.

6 cm and 12 cm above the sensing SQUID shown in figure 1. In addition, the gradiometer is mounted in a fiberglass liquid dewar to avoid the eddy-current disturbances. The SQUIDs can be operated at 77 K for about three days without refilling the liquid nitrogen. The dewar was mounted in a stable and rigid holder, which allows us to manually adjust vertical position of the dewar to make sure the sensing SQUID is close to the thorax of the human body.

2.2 Analog Subtraction Circuit

Figure 2 shows the schematic diagram of the cryostat and the SQUID electronics of magnetocardiography measurement system. The output signals of three SQUID magnetometers were fed to an analog subtraction circuit to reject the ambient noise disturbances. The subtraction instrument contains seven adjustable knobs for us to vary the gain of each output in this circuit. The output, Δ, of the 2nd-order gradiometer is

$$\Delta = [aX-e(bY)] - g[cY -f(dZ)]$$
$$= AX + BY + CZ, \qquad (1)$$

in which $A = a$, $B = -(eb + gc)$, and $C = gfd$. In our design of the analog subtraction circuit, the value of the gain a, b, c, and d can be varied from 0.5 to 1 while the value of gain e, f, and g designed to vary from 0.33 to 1.

In general, the ambient magnetic noise is composed of different disturbances with distinct frequency component in space. Furthermore, these electromagnetic disturbances are not homogeneously distributed in space. Therefore, the noises cannot fully be eliminated by the 2nd-order gradiometer. Practically, we have to specify the frequency band for choosing optimal coefficients to minimize the ambient noises.

First, we acquire the signals of three magnetometers simultaneously via the data acquisition card. Then, we apply the fast Fourier Transform (FFT) to the three signals with the Hanning window overlapped. We obtained the field spectrums that include both the real and the imaginary parts, from the three magnetometers. Since the fast Fourier transformation obeys the associative law for addition and multiplication, therefore, from Eq. (1) the FFT of Δ becomes
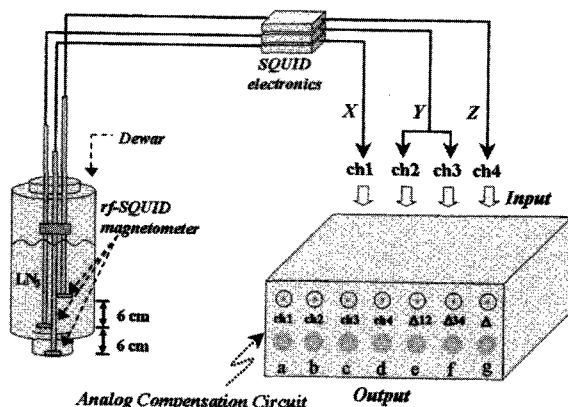

Figure 2 Schematics of the analog subtraction electronics

$$F(\Delta) = A\,F(X) + B\,F(Y) + C\,F(Z), \qquad (2)$$

The magnitude of the Fourier field spectrum of the 2nd-order gradiometer, Δ would be

Magnitude of $F(\Delta) = [\mathrm{Re}F(\Delta) + \mathrm{Im}F(\Delta)]^{1/2}$, (3)

in which $\mathrm{Re}F(\Delta)$ is the real part of $F(\Delta)$ and $\mathrm{Im}F(\Delta)$ is the imaginary part of $F(\Delta)$. We wrote a software program to search all the attainable values of the coefficients A, B, and C to minimize the magnitude of $F(\Delta)$ in the frequency band of interest. By setting $A = 1$, it is found that the optimal values are usually $B \approx -1$ and $C \ll 1$ respectively in our laboratory. The result $B \approx -1$ implies that the noise level is almost minimized with the first order gradiometer. The small value of C indicates that the small compensation from the reference SQUID Z can further improve the noise level of the first order gradiometer.

To investigate the degree of the similarity between two SQUID signals of the environment, we define the coherence function γ. As mentioned above, the FFT of the output from each channel contains both real and imaginary parts. Thus we define the coherence function from the auto-power spectrum and the cross power spectrum of the signals. The auto-power spectrum is defined as $G_{xx} = X(f)X'(f)$, where G_{xx} is the auto-power function for the signal X, $X(f)$ is the FFT of the signal X, $X'(x)$ is the complex conjugate of $X(f)$, and f is the frequency. [9] Similarly, we define the auto-power spectrum of the signal Y as $G_{yy} = Y(f)Y'(f)$, and the cross power spectrum as $G_{xy} = X(f)Y'(f)$, where $Y(f)$ is the FFT of the signal Y, and $Y'(f)$ is the complex conjugate of $Y(f)$. The coherence function, γ, is defined as:

$$\gamma^2 = \mathrm{Re}\left[\frac{|G_{xy}|^2}{G_{xx}G_{yy}}\right], \qquad (4)$$

The γ has a value that is varied from zero to one for each frequency. If $\gamma =1$ at any frequency, the two signals are completely coherent, i.e. the two magnetometers detect the same phase of the magnetic signal at any frequency. By measuring the coherence function of three magnetometers, we can obtain the information about the degree of coherence of the magnetic field in space

3. RESULTS AND DISCUSSION

Figure 3 shows the field spectrum of the magnetometer and the gradiometer in unshielded environment. The upper trace is the field spectrum of ambient noise. It appears that the ambient noise is dominated by the power line disturbance. Therefore, the 60 Hz spike, is approximately 30 $nT/Hz^{1/2}$, is much stronger than the other frequency component. Furthermore, the field noise at 1 Hz is about 1 $nT/Hz^{1/2}$. The lower trace is the output of the 2nd-order gradiometer in unshielded environment. Since the coefficients, which we chose to subtract the signals, were primarily used to eliminate the ambient noise in the frequency band below 10 Hz, the 60 Hz spike was attenuate to about 2.4 $nT/Hz^{1/2}$. Moreover, the field
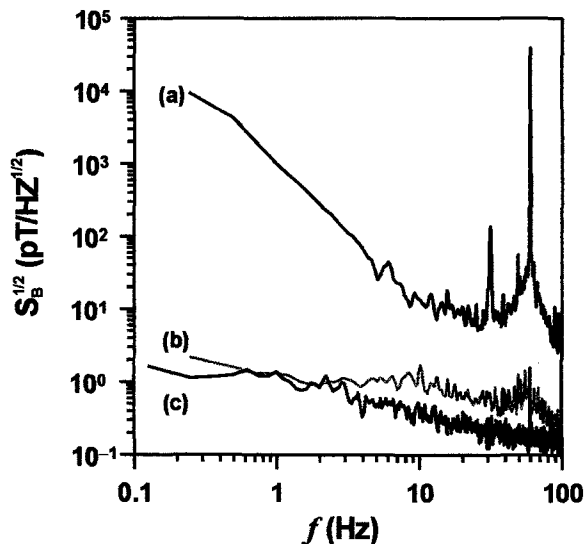
Figure 3   Magnetic field noise spectrum of (a) Unshielded   magnetometer;   (b)   Electronic gradiometer with 60 Hz notch filter and a low-pass filer in unshielded environment and (c) Shielded magnetometer

noise at 1 Hz is much reduced, about 7 $pT/Hz^{1/2}$.

As shown in Figure 3, the magnetic noise was still dominated by the power line source. Furthermore, since the field is not homogeneous in our laboratory, it cannot be fully eliminated by the 2nd-order gradiometer. Hence, the output signals of the gradiometer were further filtered through a notch filter of the power line frequency and a low-pass filter with the cutoff frequency of 30 Hz. By means of filtering, the ambient noise was further reduced. As shown in Figure 3, the 60 Hz spike was suppressed from 40 $nT/Hz^{1/2}$ to about 1 $pT/Hz^{1/2}$, i.e. the attenuation factor is about 4×10^4.

The ambient noise cannot be eliminated completely because the noises measured by three magnetometers are not perfectly correlated in the frequency band of interest. The magnetic sources far from the system may be detected simultaneously by the three magnetometers. However, the three magnetometers may detect different magnitude and phase of the magnetic sources adjacent to the system. This means that the more similar the magnetic field detected by the three magnetometers, the more effective the 2nd-gradiometer suppress the ambient noise.

Figure 4(a) shows the coherence function between SQUID X and SQUID Y while Figure 4(b) shows the coherence function between SQUID X and SQUID Z. It was found that the coherence functions were different at each frequency. The coherence between the SQUID X and the SQUID Y is better than the coherence function between SQUID X and SQUID Z. The better coherence between SQUID X and SQUID Y is due to the shorter distance is between them. The worse coherence between SQUID X and SQUID Z is responsible for the small compensation coefficient C found in the optimization of the noise of the second order gradiometer system. Besides, the magnitude of the coherence function between each channel is approximately equal to 1 at 60 Hz, the power line frequency. The result indicates that the power line disturbance distributes almost uniformly
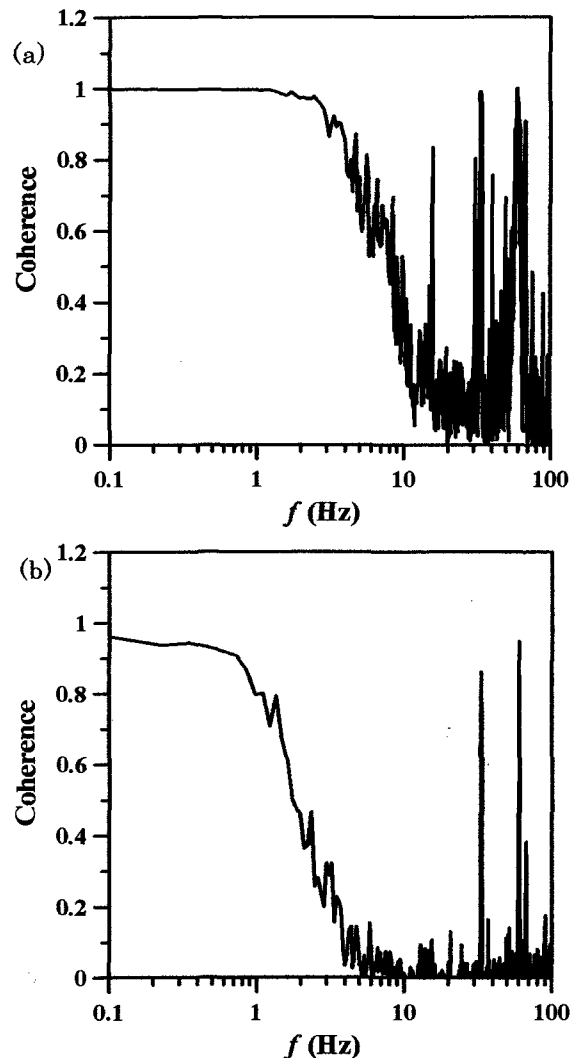

Figure 4 (a) Coherence function as a function of frequency between SQUID X and SQUID Y and (b) Coherence function as a function frequency between SQUID X and SQUID Z.

in our laboratory and all the three magnetometers detect it. The coherence was very poor between different channels at the frequency around 20 Hz due to different field distribution in the environments. That is why we cannot completely eliminate the ambient noise by the 2nd-order gradiometer in such environment.

As the noise level was lower than the typical value of MCG signals, we performed the MCG measurement in our laboratory without magnetic shielding. Figure 5 shows the averaged MCG signals over 90 heartbeats of a healthy person. By means of the averaging process, the peak-to-peak noise of the average result is about 3 pT, much smaller than the real time signal. Besides, the QRS complex wave and the T wave can be clearly seen in the averaging signal.

One goal of the MCG measurements is to demonstrate the spatiotemporal magnetic field distribution above the thorax of a person in unshielded environment. We used a single-channel gradiometer to detect the MCG signal at many distinct locations above the thorax of subject by moving the couch. The couch is equipped with computer-controlled X-Y stage permitting one to control

Figure 5 Averaged MCG signals measured at 36-points on the sensing plane above the thorax of the subject.

precisely the horizontal displacements of the person along two orthogonal directions. Figure 5 demonstrates a time-domain magnetic map of the heart activity for 36 different sites (6×6 rectangular grid with each position spaced by 4 cm) above the chest of a healthy person. With this technique we have successfully taken a two-dimensional MCG images over the chest of a healthy person in unshielded environments [5].

4. CONCLUSION

We established the FFT technique to eliminate the environmental noises of unshielded magnetocardiography imaging system. The 60 Hz spike was suppressed from 40 nT/Hz$^{1/2}$ to about 1 pT/Hz$^{1/2}$, i.e. the attenuation factor is about 4×10^4. We further demonstrate a time-domain magnetic map of the heart activity for 36 different sites (6×6 rectangular grid with each position spaced by 4 cm) above the chest of a healthy person. Besides, the performance of the off-axis gradiometer is the same as the co-axial gradiometer. We therefore use one or two SQUID magnetometers in arbitrary locations to provide reference signals and the system cost could be greatly reduced in the off-axis design.

REFERENCES

[1] Y. Tavrin, Y. Zhang, Y. Mück, A.I. Braginski and C. Heiden, *Applied Physics Letters*, 62, 1824-26 (1993).
[2] Y. Tavrin, Y. Zhang, W. Wolf and A.I. Braginski, *Superconductor Science and Technology*, 7, 265-68 (1994).

[3] Y.Zhang, G. Panaitov, S.G. Wang, N. Wolters, R. Otto, J. Schubert, W. Zander, H.-J Krause, H. Soltner, H. Bousack, and A.I. Brazinski, *Applied Physics Letters*, 76, 906-08 (2000).
[4] J. Borghann, P. Davis, G. Ockenfuss, R. Otto, J. Schubwert, W. Zander, and A.I. Brazinski, *Review of Scientific Instrument*, 68, 2730-34 (1997).
[5] H. C. Yang, S. Y. Wang, J. T. Jeng, J. H. Chen, and H. E. Horng, *IEEE Transactions on Applied Superconductivity*, 13, 360-63 (2003).
[6] H. E. Horng, S. Y. Hung, J. T. Jeng, S. H. Liao, S. C. Hsu, J. C. Hwang, and H. C. Yang, *IEEE Transactions on Applied Superconductivity*, 13, 381-84 (2003).
[7] M. Matsuda, S. Ono, K. Kato, T. Matsuura, H. Oyama, A. Harano, S. Kuriki, and K. Yokosawa, *IEEE Transactions on Applied Superconductivity*, 11, 1323-26 (2001).
[8] S. Kuriki, H. Oyama, A. Hayashi, S. Hirano, T. Washio, M. Matsuda, and K. Yokosawa, *IEICE Trans. Electron*, E85-C, 670-76 (2002).
[9] HP3562A Dynamic Signal Analyzer Operating Manual, Hewlett-Packard Co., USA., Sep., 1986.